Effect of temperature on the performance of CuPc/C_{60} photovoltaic device

2009 J. Phys. D: Appl. Phys. 42 015102

(http://iopscience.iop.org/0022-3727/42/1/015102)

IOP PUBLISHING JOURNAL OF PHYSICS D: APPLIED PHYSICS

J. Phys. D: Appl. Phys. **42** (2009) 015102 (6pp) doi:10.1088/0022-3727/42/1/015102

Effect of temperature on the performance of CuPc/C_{60} photovoltaic device

Hemant Kumar, Pankaj Kumar[1], Neeraj Chaudhary, Ramil Bhardwaj, Suresh Chand, S C Jain and Vikram Kumar

Centre for Organic Electronics, National Physical Laboratory, Dr K S Krishnan Road, Pusa, New Delhi-110012, India

E-mail: pankaj@mail.nplindia.ernet.in

Received 30 September 2008, in final form 24 October 2008
Published 4 December 2008
Online at stacks.iop.org/JPhysD/42/015102

Abstract

We demonstrate the effect of temperature on the performance of a copper phthalocyanine (CuPc)/fullerene (C_{60}) based bilayer organic photovoltaic device. The current–voltage (J–V) characteristics of the device have been studied in the dark as well as under illumination at different temperatures in the range 300–125 K. The variation in temperature strongly influences the device parameters and hence its performance. It has been found that (i) the lowering of the temperature results in a reduction in the rectification ratio, (ii) reverse bias current at low temperatures is governed by the tunnelling of the charge carriers and (iii) short circuit current (J_{sc}) decreases while the open circuit voltage (V_{oc}) increases with the decrease in temperature. The change in V_{oc} with temperature has been attributed to the variation in the built-in voltage (V_{bi}) arising due to band bending with a decrease in temperature. In summary the overall efficiency of the device first increases and then decreases with the reduction in temperature.

(Some figures in this article are in colour only in the electronic version)

1. Introduction

Organic semiconductors have emerged as revolutionary materials for their potential applications in electronic devices such as light emitting diodes, display devices, photovoltaic devices, thin film transistors and lasers [1–5]. These materials have inherent advantages for thin, low cost, light weight, flexible and large area device production and are capable of replacing bulky and costly electronic devices based on the inorganic ones. Fast and intensive research in this area has resulted in the commercialization of organic light emitting diodes and full colour displays. Elaborate research is also being done on organic photovoltaic (OPV) devices as they are one of the most promising alternative sources of energy compared with conventional energy sources [5]. The performance of OPV devices has improved considerably in the last few years by the use of better absorbing materials, new device architectures and different thermal and field treatments [6–8]. The power conversion efficiency (η) of ~6.5% has successfully been realized in tandem OPV devices based on a polymer : fullerene interpenetrating bulk heterojunction network [7]. Stability is one of the major concerns for these devices; therefore, intensive research is also being done worldwide to improve the stability of OPV devices [9, 10]. Jorgensen *et al* gave an excellent review on the degradation and stability of OPV devices and the report is presented in [11]. Because of continuous efforts and hard work of the researchers, OPV devices having an outdoor lifetime of several thousand hours have successfully been fabricated [12–14]. Easy processability for large area devices fabrication is also one of the biggest driving forces for the development of OPV devices [14, 15]. Kerebs *et al* have fabricated large area flexible plastic solar cell modules of size ~0.1 m^2 and the results are reported in [15]. The η of a solar cell depends on the open circuit voltage (V_{oc}), short circuit current (J_{sc}) and fill factor (FF) as

$$\eta = \frac{J_{sc} V_{oc} FF}{P_{in}}, \tag{1}$$

where P_{in} is the incident optical power. FF depends on the series resistance and determines the shape of the characteristics. Under light illumination the absorbed light photons generate excitons, which diffuse to the donor–acceptor interface and dissociate there. The efficient dissociation

[1] Author to whom any correspondence should be addressed.

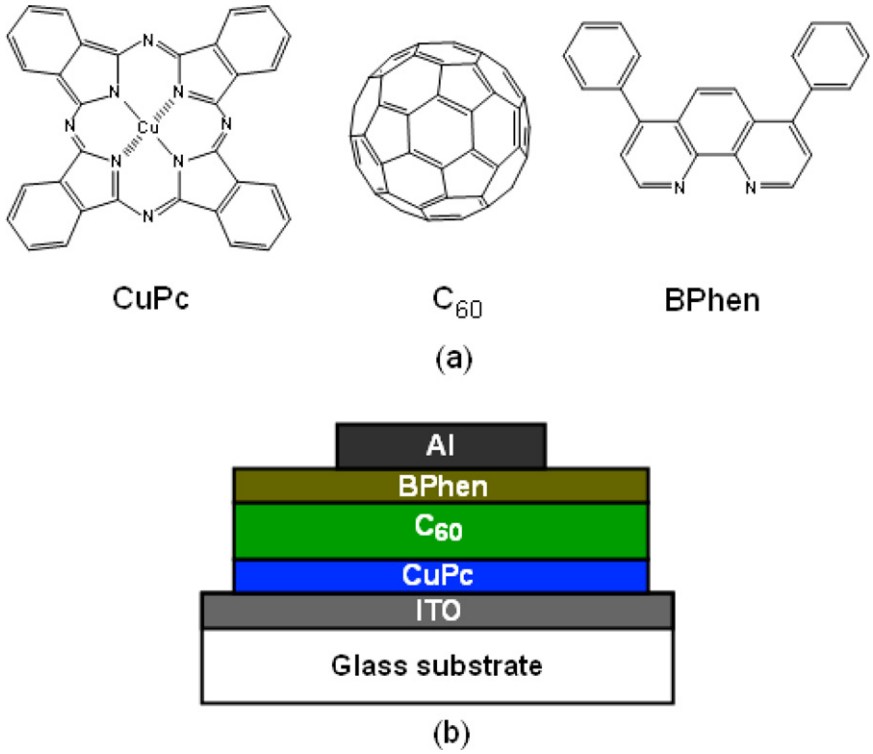

Figure 1. (*a*) Molecular structure of the materials used and (*b*) schematic structural diagram of the device.

of photo-generated excitons and rapid transportation of the separated charge carriers through the two different layers result in high efficiency in these devices. Copper phthalocyanine (CuPc) and fullerene (C_{60}) are, respectively, the most important small molecular donor and acceptor materials for OPV applications and $\eta \sim 5.58\%$ has already been achieved for the CuPc/C_{60} system [6]. For the reliability of these devices in different conditions it is very important to investigate the effect of various physical parameters such as temperature, humidity, electric/magnetic field and illumination intensity on their performance. For this purpose we have investigated the effect of temperature on the performance of CuPc/C_{60} based bilayer OPV devices and the results of the same are reported here. These studies have been carried out both in the dark and under illumination. The variation in temperature has been found to have a significant effect on J_{sc}, V_{oc}, FF and η of the device. This paper attempts to elucidate the mechanism governing the charge carrier transport and generation of photocurrent/photovoltage in the OPV devices and the effect of temperature on them.

2. Experimental details

The OPV device under study has been fabricated in the bilayer configuration, namely, indium tin oxide (ITO)/CuPc/C_{60}/batho-phenanthroline (BPhen)/Al where ITO, CuPc, C_{60}, BPhen and Al are, respectively, the anode, electron donor, electron acceptor, exciton blocking and cathode materials. The application of exciton blocking layers in the OPV devices has proved to be quite efficient as it prevents exciton diffusion and their subsequent quenching at the organic–metal cathode interface [16, 17]. Though the devices under study have been fabricated on the ITO coated glass substrates (sheet resistance $\sim 18\,\Omega/\square$), it is worth reporting that ITO has no future in low cost solar cells and suitable alternatives have to be found. Some alternatives have been found by the researchers [18–20] and the search for more suitable alternatives is going on. The ITO substrates used in these studies were patterned and cleaned properly via the standard cleaning process. Prior to any deposition the ITO substrates were exposed to oxygen plasma for 5 min and then transferred to a vacuum chamber, where thin film depositions of CuPc (20 nm), C_{60} (40 nm), BPhen (8 nm) and Al (150 nm) were carried out via thermal evaporation of the materials at the base pressure $\sim 7\times10^{-6}$ Torr. All the materials were purchased from Sigma-Aldrich USA and were used as such. The rate of evaporation of these materials was monitored using an oscillating quartz crystal and maintained between 0.1 and 0.4 Å s^{-1} for organics and 1 and 2 Å s^{-1} for Al. An Al cathode was deposited through the shadow mask, which defined the active area of the device to be 0.12 cm^2. Figures 1(*a*) and (*b*), respectively, show the molecular structures of the materials used and the schematic structural diagram of the device. The device was transferred to a laboratory-made low temperature measurement assembly, where the J–V characteristics were carried out in the dark and under illumination. A 1000 W halogen lamp from OSRAM, Germany, was used to illuminate the cell. The intensity of the lamp was calibrated and adjusted for 80 mW cm^{-2} using a standard Si solar cell from PV Measurements Inc. US, and a Solar Simulator from Oriel USA. A Keithley 2400 Source-Measure unit, interfaced with the computer, was used to measure the J–V characteristics.

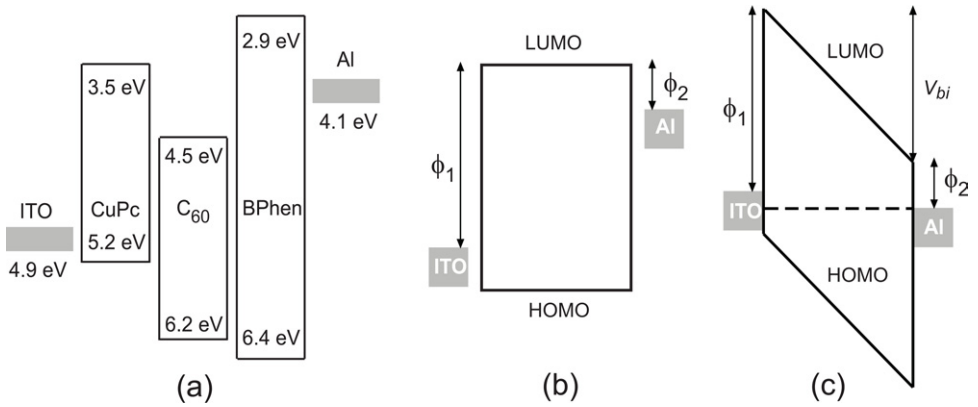

Figure 2. Schematic energy level diagrams of the device (*a*) when the materials have not been brought into close contact, (*b*) when the active organic layer is assumed to be a single semiconductor and (*c*) when the materials are brought into close contact.

3. Results and discussion

The OPV devices contain the structure of an active organic layer sandwiched between two metal electrodes (generally ITO and Al). When a semiconductor is sandwiched between two electrodes of different work functions Fermi level alignment takes place and electrons diffuse from the cathode to the anode. This diffusion of the electrons results in the development of an electric field in the device and this electric field is known as the built-in electric field. The corresponding voltage developed between the two electrodes is known as the built-in voltage (V_{bi}). Figure 2(*a*) shows the schematic energy level diagram of the materials used before they are brought into close contact. For simplicity of understanding of device physics, the whole of the organic active layer has been assumed to be a single semiconductor. The energy level diagram of the system can now be shown to be schematic as in figure 2(*b*). When the materials are brought into close contact to fabricate the device Fermi level alignment takes place and the energy level diagram in this case is shown in figure 2(*c*). It is clear from figure 2(*c*) that V_{bi} is the voltage which is required for the flat band condition to occur.

Figure 3 shows the dark J–V characteristics of the device measured at different temperatures in the range 300–125 K. The current density is observed to decrease continuously with lowering of the temperature in the forward bias (+ve voltage to ITO), while in the case of reverse bias (+ve voltage to Al) the current has been found to decrease when the temperature was lowered from 300 to 210 K. However, further reduction in temperature had almost no effect on the current and it becomes almost independent of the temperature. It is seen from figure 3 that the reduction in the reverse current is relatively low compared with that in the forward current. At 300 K the device showed typical diode characteristics with a rectification ratio of 2.98×10^2 at ± 1 V which reduced to 5.5 at ± 1 V at 125 K. The temperature independence of the current below 210 K in the reverse bias suggests that a different charge transport phenomenon takes place below this temperature. To understand the physics of characteristics in the reversed bias, J–V characteristics measured at 300 and 210 K have been plotted separately in figure 4. Symbols represent the experimental data. The characteristics measured

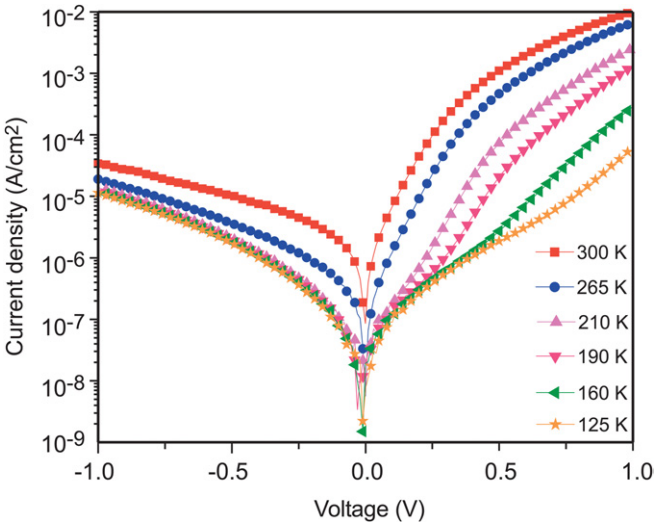

Figure 3. J–V characteristics of the ITO/CuPc(20 nm)/C_{60}(40 nm)/Bphen(8 nm)/Al solar cell in the dark at different temperatures.

below 210 K are very similar to that measured at 210 K; therefore, the results below 210 K have not been plotted in figure 4. It has been found that the characteristic at 300 K follows Ohmic behaviour ($J \propto V$) which can presumably be attributed to the very high injection barriers for charge carriers [21] in reverse bias. The solid curve represents Ohm's law. However, at low temperatures the situation changes. At low temperatures charges do not have sufficient energy to overcome [22] the injection barriers and therefore are injected into the semiconductor via tunnelling through the barriers (see figure 5(*a*)). The dashed curve in figure 4 represents $J \propto F^2 \exp(-B/F)$, which corresponds to the tunnelling of the charge carriers [23] through the injection barrier. Here F is the electric field and B is a constant. It is thus established that the reverse bias current in the present OPV device is governed by the tunnelling mechanism at low temperatures.

V_{bi} plays an important role in the determination of the J–V characteristics in the forward bias. Mihailetchi *et al* [24] have shown that the dark J–V characteristics of an OPV device contain two important regimes. (i) $V < V_{bi}$, where the built-in electric field opposes the direction of the current and current

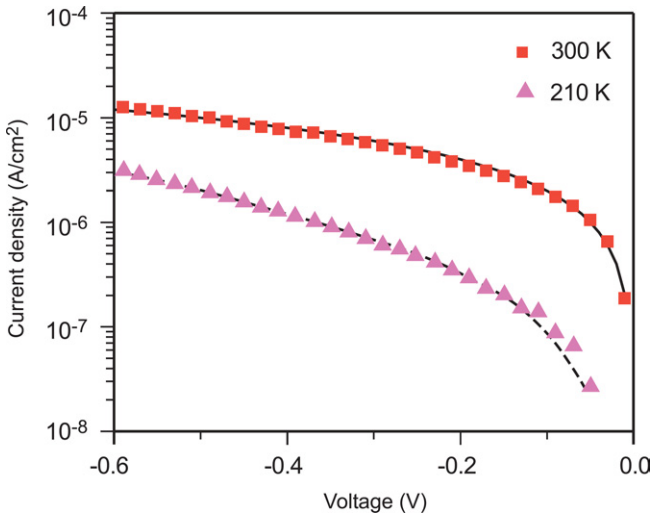

Figure 4. Reverse biased J–V characteristics of the ITO/CuPc(20 nm)/C_{60}(40 nm)/Bphen(8 nm)/Al solar cell at 300 and 210 K. Symbols represent the experimental data while solid and dashed curves represent, respectively, the Ohmic and tunnelling currents.

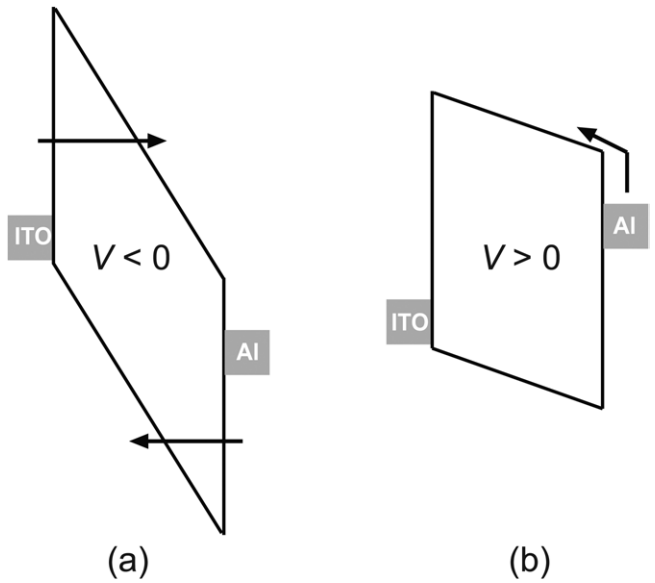

Figure 5. Schematic representation of the device in (*a*) reverse bias and (*b*) forward bias conditions.

is dominated by the diffusion of charge carriers. The charge carriers are injected into the energy band of the semiconductor due to thermionic emission and diffuse to the other electrode (see figure 5(*b*)). In this regime current increases exponentially with the applied voltage. (ii) $V > V_{bi}$, in this case the flat band condition is reached and the current is now governed by space charge limited conduction (SCLC). Since the charge density in the vicinity of the metal contact is much higher than the densities associated with SCLC, it is reasonable to consider the onset of SCLC occurs when the flat band condition is reached. In the case of the flat band condition, large numbers of authors have reported SCLC in organics [25–28]. Similarly to Mihailetchi *et al* [24], the current for $0 < V < V_{bi}$ and $V > V_{bi}$ in our experimental results as well

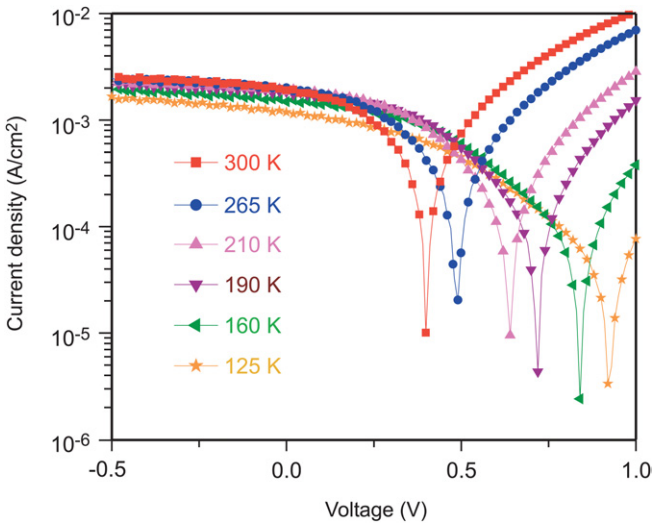

Figure 6. J–V characteristics of the ITO/CuPc(20 nm)/C_{60}(40 nm)/Bphen(8 nm)/Al solar cell under 80 mW cm^{-2} irradiance of halogen lamp at different temperatures.

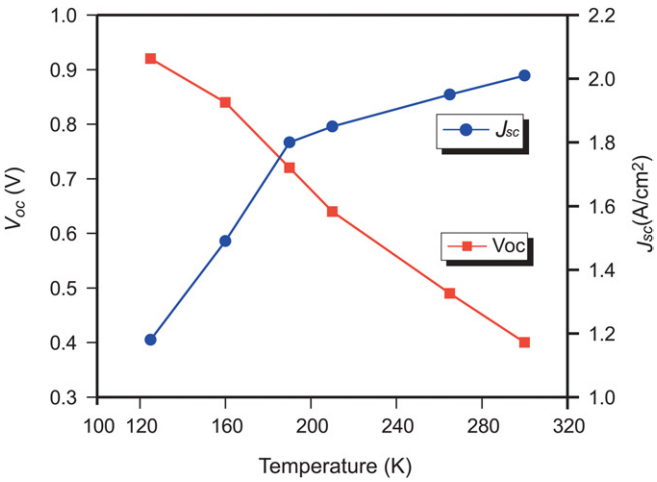

Figure 7. Variation of V_{oc} and J_{sc} as a function of temperature.

can, respectively, be attributed to the diffusion and SCLC of charge carriers.

Figure 6 shows the illuminated J–V characteristics of the device at different temperatures on a semi-log scale. It is observed that the current decreases with the reduction in temperature. However, the reduction in current with temperature in reverse bias has been observed to be very slow compared with the one in the forward bias case. The effect of temperature on J_{sc} and V_{oc} is shown in figure 7. It is observed that J_{sc} decreases while V_{oc} increases almost linearly with the lowering of temperature. Organic semiconductors are generally amorphous in nature and contain traps. The strong temperature dependence of J_{sc} can be attributed to the electronic transport properties of the light absorbing material. Their charge carrier mobilities are very low and depend on the temperature. Furthermore, it is negatively influenced by the capture of charge carriers by traps. One would expect that the lowering of temperature will reduce the current [5]. Therefore, the reduction in J_{sc} can be interpreted in terms of

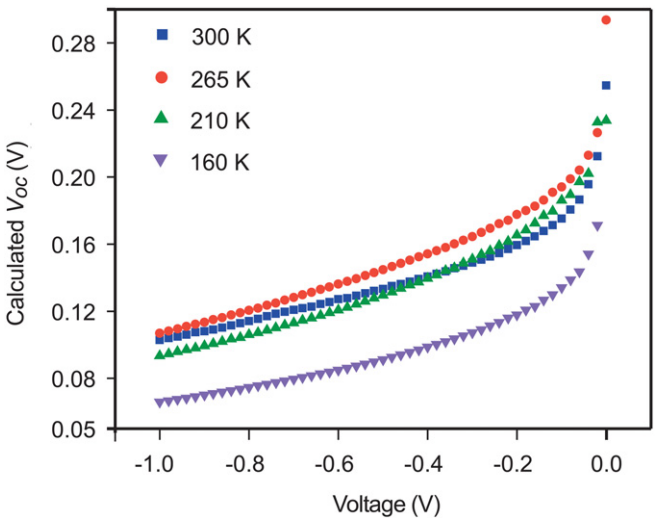

Figure 8. Variation of the calculated V_{oc} (using equation (2)) with the applied voltage at different temperatures. Note that just for the study of the behaviour of V_{oc} we replaced J_0 by the reverse bias current in equation (2).

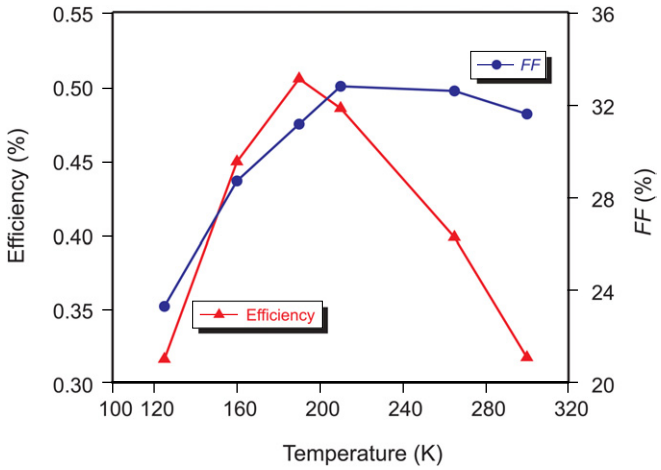

Figure 9. Variation of FF and η as a function of temperature.

the trapping effect and the reduction in charge carrier mobility with temperature.

The origin of V_{oc} in OPV devices is not clearly understood and has been attributed to various mechanisms. It has usually been suggested that V_{oc} in OPV devices depends either on the difference in the energies of HOMO of the donor and LUMO of the acceptor [29, 30] or on the difference in the work functions of the anode and the cathode used [24] or modification in the interface barriers due to interface layer treatments, etc. The variation of V_{oc} with temperature in the present case makes it difficult to explain its origin explicitly. In conventional Si solar cells the temperature dependence of V_{oc} is given by

$$V_{oc} = \frac{nkT}{q} \ln\left(\frac{J_{sc}}{J_0} + 1\right), \qquad (2)$$

where J_0 is the reverse saturation current in the device and n is the diode ideality factor. Equation (2) has also been used to explain the V_{oc} in OPV devices [31]. In the present case we do not observe saturation in the reverse bias current; hence equation (2) cannot explain our experimental results. However, even assuming that saturation may occur at very high voltages we have plotted V_{oc} in figure 8 , calculated using equation (2) and our experimental data. Note that just for understanding the behaviour of V_{oc} we replaced J_0 by the reverse bias current in equation (2). Symbols in figure 8 represent the calculated V_{oc} as a function of the applied voltage at different temperatures. For these calculations n has been taken to be 1. Figure 8 shows that even at high voltages the V_{oc} first increases and then decreases with temperature. If the curves in figure 8 are additionally plotted to very high voltages the V_{oc} attains very low values. These results are quite contrary to the observed results; therefore, we conclude that equation (2) is not suitable for our experimental data.

Alternatively the temperature dependence of the V_{oc} in the present case has been attributed in terms of the temperature dependence of V_{bi}. For the devices containing significant V_{bi}, diffusion plays an important role and may cause a significant charge carrier density in the entire device. Incorporation of an optimized thickness of the exciton blocking layer provides the Ohmic contact to the electron injection [32, 33]. We have studied the effect of thickness of BPhen on the performance of CuPC/C_{60} photovoltaic devices and the results are under publication [17]. The optimum thickness of BPhen for the best device performance is observed to be 8 nm. In the present studies as well the electron injection contact may be assumed to be Ohmic. Mihailetchi *et al* [24] showed that in the vicinity of the Ohmic contact a significant band bending occurs due to accumulation and diffusion of charge carriers. This band bending produces a significant loss in the V_{bi}. Kemerink *et al* [34] used a simple analytical model to study the effect of temperature on band bending. It has been shown that band bending at the electrodes depends upon temperature and decreases with the lowering in temperature. The reduction in band bending with temperature directly reflects the decrease in the diffusion coefficient, leading to a reduction in curvature of the band edge. The reduction in band bending at low temperatures results in the increment in V_{bi}. It is well known that V_{oc} has a direct dependence on V_{bi}. Therefore the reduction in temperature results in the increment in V_{oc}.

Figure 9 shows the variation of FF and η with temperature. The observed temperature dependence of FF is similar to that of J_{sc}. This behaviour can be qualitatively understood in terms of the temperature dependent series resistance of the OPV devices. In the case of inorganic semiconductors the resistivity of the active semiconductor material is very low and the series resistance is solely determined by the metal–semiconductor interface and is independent of the temperature. On the other hand, OPV devices have relatively high resistivity of the organic active layers (bulk resistivity) that increases with decreasing temperature. The increase in resistivity with the decrease in temperature can be attributed to the trapping effect and lowering of the charge carrier mobilities. It is this increase in resistivity which reduces the FF with the lowering in temperature. As regards the efficiency it increases first and then decreases with the decrease in temperature. The variation of efficiency with temperature can be understood from equation (1). At relatively higher temperatures (>200 K)

the reduction in the value of the $J_{sc} \times$ FF factor is less compared with the corresponding increase in V_{oc}; therefore, the efficiency has a negative temperature coefficient and increases with the reduction in temperature. However, at low temperatures (<200 K) strong temperature dependence of $J_{sc} \times$ FF overwhelms the weak temperature dependence of V_{oc} and η has a positive temperature coefficient. Therefore η decreases with further reduction in temperature.

4. Conclusion

The effect of temperature on the performance of the CuPC/C_{60} based OPV device has been investigated and it has been found that the lowering in temperature plays a significant role in device performance. It has been established that the dark current under reverse bias and at low temperatures is governed by the tunnelling of the charge carrier mechanism whereas under forward bias it is first dominated by diffusion for $V < V_{bi}$ and then by SCLC at $V > V_{bi}$. J_{sc} decreases while V_{oc} increases with the reduction in temperature. The reduction in J_{sc} has been attributed to the trapping effect and reduction in charge carrier mobility with temperature. The increment in V_{oc} has been attributed to the increment in V_{bi} due to reduction in bend bending with the lowering in temperature. The overall efficiency of the device increases first and then decreases with lowering of the temperatures and it has been attributed to the dominance and vice versa of the V_{oc} on the product $J_{sc} \times FF$.

Acknowledgment

The authors would like to thank Dr S S Bawa, Dr A K Gupta, Mr Sudhansu Dwivedi and Mr G D Sharma for their help and support. One of them (HK) is grateful to CSIR, India, for awarding the Junior Research Fellowship.

References

[1] Misra A, Kumar P, Kamalasanan M N and Chandra S 2006 *Semicond. Sci. Technol.* **21** R35
[2] Bundgaard E and Krebs F C 2007 *Sol. Energy Mater. Sol. Cells* **91** 954
Spanggaard H and Krebs F C 2004 *Sol. Energy Mater. Sol. Cells* **83** 125
[3] Gunes S, Neugebauer H and Sariciftci N S 2007 *Chem. Rev.* **107** 1324
Brabec C J, Sariciftci N S and Hummelen J C 2005 *Adv. Funct. Mater.* **11** 15
[4] Sirringhaus H 2005 *Adv. Funct. Mater.* **17** 2411
[5] Jain S C, Willander M and Kumar V 2007 *Conducting Organic Materials and Devices* (San Diego, CA: Academic Press)
[6] Chan M Y, Lai S L, Fung M K, Lee C S and Lee S T 2007 *Appl. Phys. Lett.* **90** 23504
[7] Kim J Y, Lee K, Coates N E, Moses D, Nguyen T Q, Dante M and Heeger A J 2007 *Science* **317** 222
[8] Padinger F, Rittberger R S and Sariciftci N S 2003 *Adv. Funct. Mater.* **13** 85
[9] Krebs F C 2008 *Sol. Energy Mater. Sol. Cells* **92** 715
Krebs F C, Thomann Y, Thomann R and Andreasen J W 2008 *Nanotechnology* **19** 424013
Katz E A, Gevorgyan S, Orynbayev M S and Krebs F C 2006 *Eur. Phys. J. Appl. Phys.* **36** 307
[10] Yang X, Loos J, Veenstra S C, Verhees W J H, Wienk M M, Kroon J M, Michels M A J and Janssen R A J 2005 *Nano Lett.* **5** 579
[11] Jørgensen M, Norrman K and Krebs F C 2008 *Sol. Energy Mater. Sol. Cells* **92** 686
[12] Hauch J A, Schilinsky P, Choulis S A, Childers R, Biele M and Brabec C J 2008 *Sol. Energ. Mater. Sol. Cells* **92** 727
[13] Krebs F C and Spanggaard H 2005 *Chem. Mater.* **17** 5235
[14] Lungenschmied C, Dennler G, Neugebauer H, Sariciftci S N, Glatthaar M, Meyer T and Meyer A 2007 *Sol. Energy Mater. Sol. Cells* **91** 379
[15] Krebs F C, Spanggard H, Kjær T, Biancardo M and Alstrup J 2007 *Mater. Sci. Eng.* B **138** 106
[16] Noda T, Ogawa H and Shirota Y 1999 *Adv. Mater.* **11** 283
[17] Kumar H, Kumar P, Bhardwaj R, Sharma G D and Chand S at press
[18] Aernouts T, Vanlaeke P, Geens W, Poortmans J, Heremans P, Borghs S, Mertens R, Andriessen R and Leenders L 2004 *Thin Solid Films* **451–452** 22
[19] Lee J Y, Connor S T, Cui Y and Peumans P 2008 *Nano Lett.* **8** 689
[20] Jensen B W and Krebs F C 2006 *Sol. Energy Mater. Sol. Cells* **90** 123
Strange M, Plackett D, Kaasgaard M and Krebs F C 2008 *Sol. Energy Mater. Sol. Cells* **92** 805
[21] Kumar P, Jain S C, Misra A, Kamalasanan M N and Kumar V 2006 *J. Appl. Phys.* **100** 114506
[22] Sze S M 1981 *Physics of Semiconductor Devices* (New York: Wiley)
[23] Chanana R K, McDonald K, Di Ventra M, Pantelides S T, Feldman L C, Chung G Y, Tin C C, Williams J R and Weller R A 2000 *Appl. Phys. Lett.* **77** 2560
[24] Mihailetchi V D, Blom P W M, Hummelen J C and Rispens M T 2003 *J. Appl. Phys.* **94** 6849
[25] Campbell A J, Weaver M S, Lidzey D G and Bradly D D C 1998 *J. Appl. Phys.* **84** 6737
[26] Kao K C and Hwang W 1981 *Electrical Transport in Solids* (Oxford: Pergamon)
[27] Lampert M A and Mark P 1970 *Current Injection in Solids* (New York: Academic)
[28] Kumar P, Jain S C, Kumar V, Misra A, Chand S and Kamalasanan M N 2007 *Synth. Met.* **157** 905
[29] Gadisa A, Svensson M, Andersson M R and Inganas O 2004 *Appl. Phys. Lett.* **84** 1609
[30] Brabec C J, Cravino A, Meissner D, Sariciftci N S, Fromhertz T, Rispens M T, Sanchez L and Hummelen J C 2001 *Adv. Funct. Mater.* **11** 374
[31] Katz E A, Faiman D, Tuladhar S M, Kroon J M, Wienk M M, Fromherz T, Padinger F, Brabec C J and Sariciftci N S 2001 *J. Appl. Phys.* **90** 5343
[32] Peumans P and Forrest S R 2001 *Appl. Phys. Lett.* **79** 126
[33] Chan M Y, Lee C S, Lai S L, Fung M K, Wong F L, Sun H Y, Lau K M and Lee S T 2006 *Appl. Phys. Lett.* **100** 94506
[34] Kemerink M, Karmer J M, Gommans H H P and Janssen R A J 2006 *Appl. Phys. Lett.* **88** 192108